Cork Open Research Archive
Cartlann Taighde Oscailte Chorcaí

UCC Library and UCC researchers have made this item openly available. Please let us know how this has helped you. Thanks!

Title	The formation, stability, and suitability of n-type junctions in germanium formed by solid phase epitaxial recrystallization
Author(s)	Duffy, Ray; Shayesteh, Maryam; White, Mary; Kearney, John; Kelleher, Anne-Marie
Publication date	2010
Original citation	Duffy, R., Shayesteh, M., White, M., Kearney, J. and Kelleher, A.-M. (2010) 'The formation, stability, and suitability of n-type junctions in germanium formed by solid phase epitaxial recrystallization', Applied Physics Letters, 96(23), pp. 231909. doi: 10.1063/1.3452345
Type of publication	Article (peer-reviewed)
Link to publisher's version	http://aip.scitation.org/doi/abs/10.1063/1.3452345 http://dx.doi.org/10.1063/1.3452345 Access to the full text of the published version may require a subscription.
Rights	**© 2010 American Institute of Physics.This article may be downloaded for personal use only. Any other use requires prior permission of the author and AIP Publishing. The following article appeared in Duffy, R., Shayesteh, M., White, M., Kearney, J. and Kelleher, A.-M. (2010) 'The formation, stability, and suitability of n-type junctions in germanium formed by solid phase epitaxial recrystallization', Applied Physics Letters, 96(23), pp. 231909 and may be found at http://aip.scitation.org/doi/abs/10.1063/1.3452345**
Item downloaded from	http://hdl.handle.net/10468/4340

Downloaded on 2021-01-22T03:55:05Z

University College Cork, Ireland
Coláiste na hOllscoile Corcaigh

The formation, stability, and suitability of n-type junctions in germanium formed by solid phase epitaxial recrystallization

R. Duffy, M. Shayesteh, M. White, J. Kearney, and A.-M. Kelleher

Citation: Appl. Phys. Lett. **96**, 231909 (2010); doi: 10.1063/1.3452345
View online: http://dx.doi.org/10.1063/1.3452345
View Table of Contents: http://aip.scitation.org/toc/apl/96/23
Published by the American Institute of Physics

The formation, stability, and suitability of n-type junctions in germanium formed by solid phase epitaxial recrystallization

R. Duffy,[a] M. Shayesteh, M. White, J. Kearney, and A.-M. Kelleher
Tyndall National Institute, University College Cork, Lee Maltings, Cork, Ireland

(Received 29 April 2010; accepted 17 May 2010; published online 10 June 2010)

Design and optimization of n-type doped regions in germanium by solid phase epitaxial recrystallization (SPER) have been studied by the authors. A systematic study is presented of process variables that influence activation and thermal stability, including preamorphization, coimplants, recrystallization temperature, and postrecrystallization thermal treatments. Unlike silicon, activation after recrystallization in germanium is not optimum where the postrecrystallization thermal budget is kept to a minimum. With the aid of modeling, a maximum peak activation of 7×10^{19} cm^{-3} was extracted. A steady increase in sheet resistance during postrecrystallization anneals confirms the formation of metastable activation by SPER. It is predicted that active concentrations of $6-8\times10^{19}$ cm^{-3} are sufficient to meet targets for sub-20 nm technologies. © *2010 American Institute of Physics*. [doi:10.1063/1.3452345]

As germanium provides much higher carrier mobilities than silicon, interest in this semiconductor has risen sharply in recent times,[1–4] especially in the ongoing battle to boost metal-oxide-semiconductor (MOS) device drive current in advanced technologies. n-type dopants in germanium have proven to be problematic, and are now a key bottleneck in the realization of advanced n-type MOS (NMOS) device performance and scaling.[5] In short, phosphorus (P) and arsenic (As) are relatively difficult to activate and diffuse quickly,[6–9] leading to high resistances and limited capability to reduce the device dimensions.

Solid phase epitaxial recrystallization (SPER) is advantageous in this regard, as the low-temperature process limits dopant diffusion, while metastable solubility can be generated[10,11] higher than equilibrium solubility.[12,13] A low-temperature process also reduces the risk of substrate loss and dopant out-gassing, which have been flagged as critical concerns for processing germanium substrates.[14,15] SPER has recently been explored for p-type[16–18] and n-type[19,20] dopant activation in germanium but a number of key issues remain. Deactivation kinetics have been studied in silicon[21–23] but this aspect is largely unexplored at this point of time for n-type dopants in germanium. Moreover, optimization of process variables such as implants and recrystallization temperatures require fine tuning. Finally, it must be determined whether the dopant activation levels produced by SPER will be useful for future generation complementary metal-oxide semiconductor technologies.

Note that germanium is easier to amorphize than silicon,[24] possibly linked to less dynamic annealing during ion implant. Amorphization occurs even during a 5×10^{13} cm^{-2} dose P implant.[25] Consequently it is expected that n-type implants required for highly doped regions will amorphize the germanium substrate. In this work we focus on P, to be consistent with most experimental studies to date in this field.

Experiments were performed on (100) n-type germanium wafers, with bulk resistivity of 0.2–0.5 Ω cm. After a standard clean, wafers received a boron implant with a dose of 1×10^{13} cm^{-2} and energy of 60 keV, and a P implant with a dose of 1×10^{15} cm^{-2} and energy of 15 keV which amorphizes to a depth of 33 nm.[26] In some cases wafers first received a germanium preamorphizing implant (PAI) with a dose of 1×10^{14} cm^{-2} and energy of 150 keV which amorphizes to a depth of 120 nm.[27] One wafer received a fluorine (F) implant with a dose of 1×10^{15} cm^{-2} and energy of 10 keV. Finally, one wafer received only 5×10^{14} cm^{-2} P dose but had an additional As implant with the same projected range, with a dose of 5×10^{14} cm^{-2} and energy of 28 keV. All implants were performed at a tilt of 7°, with a native oxide covering the substrate. Wafers were subsequently annealed for SPER in an inert ambient for 3 min at either 400 or 500 °C. Intrinsic germanium recrystallization rates are ~2 nm/s and 200 nm/s, respectively, for these temperatures,[27] and so the SPER anneals should avoid incomplete recrystallization. All the post-SPER anneals were performed at 400 °C, in additive increments of 10, 30, 100, and 300 min. Based on the model of Ioannou *et al.*,[14] 1.3 nm of substrate loss is expected for a 400 °C 443 min anneal.

Anneal temperatures were kept in the 400–500 °C range, as P diffusion is known to occur quite rapidly already at 600 °C.[6–9] Quantifying the expected diffusion is difficult as available diffusivity values were either extracted under intrinsic conditions, or at higher temperatures than studied here.[1] However, extrapolating diffusivity values from Chui *et al.*,[6] which are accurate for high concentrations, only a few nanometers of diffusion could be expected for the highest thermal budgets in this work.

Figure 1 shows experimental sheet resistance (R_s) data as a function of implant and anneal. The data is divided into two groups, namely, those recrystallized at 400 °C and those recrystallized at 500 °C. R_s is lower when recrystallization is done at a higher temperature, which is in contrast to silicon where a low thermal budget for recrystallization is generally accepted as being the best approach. This trend was also evident in the recent results of Chao and Woo.[20] The gradual increase in R_s in Fig. 1(b) with post-SPER annealing indicates the destruction of metastable activation. It is assumed that the lack of this trend in Fig. 1(a) is due to lower

[a]Electronic mail: ray.duffy@tyndall.ie.

 © 2010 American Institute of Physics

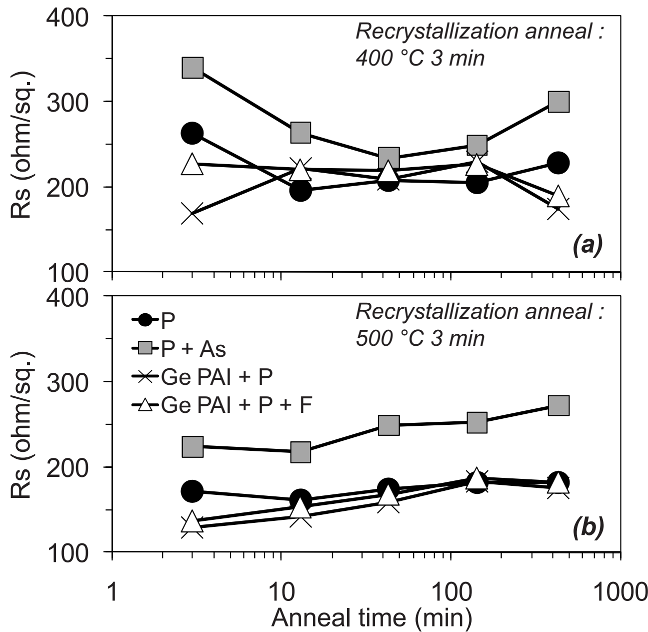

FIG. 1. Experimental R_s vs anneal time for n-type doped germanium layers. SPER was done at either 400 or 500 °C. All the post-SPER anneals were done at 400 °C.

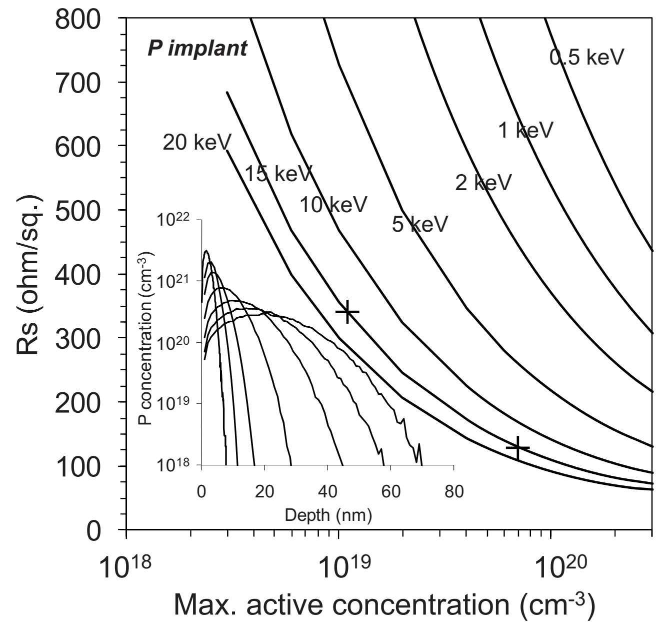

FIG. 2. Modeled R_s vs maximum active concentration for P implants with different energies, assuming concentration dependent carrier mobility. The maximum and minimum experimental data are shown on the 15 keV line. The inset shows the SRIM simulated P implant profiles.

activation created by SPER at 400 °C. The inclusion of coimplants such as PAI and F have a minor impact on the single P implant approach. Combining P with As leads to higher R_s values.

Equilibrium and metastable solubility and activation can be hindered by dopant-defect cluster formation. P tends to combine with vacancies (V) in germanium to form P_nV_m clusters.[28,29] The initial R_s value may be influenced by the formation of P_nV_m clusters or other grown-in complexes in amorphous germanium. Formation of vacancy-rich clusters is known to occur in amorphous silicon, as F_nV_m clusters can nucleate during SPER.[30] Higher SPER temperature could limit the formation of these clusters and complexes. Using even higher temperatures (>500 °C) may not provide an added benefit, as for the *same* P implant (1×10^{15} cm^{-2}, 15 keV), high-temperature flash[31] and laser[26] anneal do not beat SPER at 500 °C in terms of the R_s versus junction depth (X_j) tradeoff.

Deactivation kinetics in post-SPER silicon have been linked to interstitials (I) emitted from the end-of-range (EOR) defect band interacting with the dopant atoms, and the formation of dopant-defect clusters, the rate of which depends on the thermal budget of the postanneals,[21] the location of the EOR band with respect to the dopant,[22] and the presence or not of a coimplanted nondopant species.[23] In germanium, the EOR defects are relatively short lived and do not necessarily follow a classical Ostwald ripening process.[27] However, due to the greater likelihood of P_nV_m cluster formation, rather than P_nI_m formation, the thermal stability of the activated profile largely depends on the vacancy population, which often relies on thermal generation and injection from surfaces. Techniques that control these processes need future exploration.

In order to interpret the R_s data more thoroughly and evaluate the activation levels generated by SPER, modeling was undertaken using The Stopping and Range of Ions in Matter (SRIM).[32] P implants with 1×10^{15} cm^{-2} dose were modeled with energies ranging from 0.5 to 20 keV, shown in the inset of Fig. 2. R_s is defined as $R_s=1/\int_0^{X_j} q\mu N_D dx$, where X_j is junction depth, q is electronic charge, μ is electron mobility and is a function of active donor concentration, N_D. Using the mobility data of Fistul *et al.*[33] R_s was extracted for each implanted profile for varying N_D, assuming a diffusionless anneal. Figure 2 shows that R_s decreases with increasing N_D and implant energy as expected. The lowest and highest experimental R_s values extracted, namely, 128.9 and 336.9 Ω/sq are plotted on the 15 keV trend line in Fig. 2. From this plot we can extract the corresponding active levels of 7×10^{19} cm^{-3} and 1.1×10^{19} cm^{-3}, respectively.

This analysis can be more useful by considering the R_s versus X_j tradeoff. Assuming an extended planar bulk architecture, channel concentration increases with MOS device and junction scaling. For the P profiles of Fig. 2, in accordance with specs in the ITRS Roadmap 2000–2009 editions,[34] X_j is the depth at concentrations of 5×10^{18} cm^{-3}, 2.5×10^{18} cm^{-3}, and 1×10^{18} cm^{-3}, for the 0.5–2 keV, 5–10 keV, and 15–20 keV profiles, respectively. R_s versus X_j is plotted in Fig. 3, in the form of constant N_D contour lines. The corresponding P implant energies are included on the x-axis. ITRS Roadmap target specs are added from the 2009 and 2003 editions. The 2009 edition specs are more relevant as those are the targets that industry is shooting for at this point in time. However, due to the lack of development of scaled implanted n-type junctions in germanium, to date published R_s versus X_j data is limited to X_j >60 nm.[26,31,35] 2003 specs are a useful guide as they concern junctions with X_j=28–75 nm. The afore-mentioned flash and laser anneal data are also shown in Fig. 3.[26,31] Note Heo *et al.*[36] reported R_s versus X_j data with X_j<60 nm, by combining PH_3 plasma doping with laser anneal.

According to the ITRS, R_s is a designated percentage of total source-drain resistance (R_{SD}). While R_s is not specified for different device options, R_{SD} is defined with the same value for high performance (HP), low-operating power

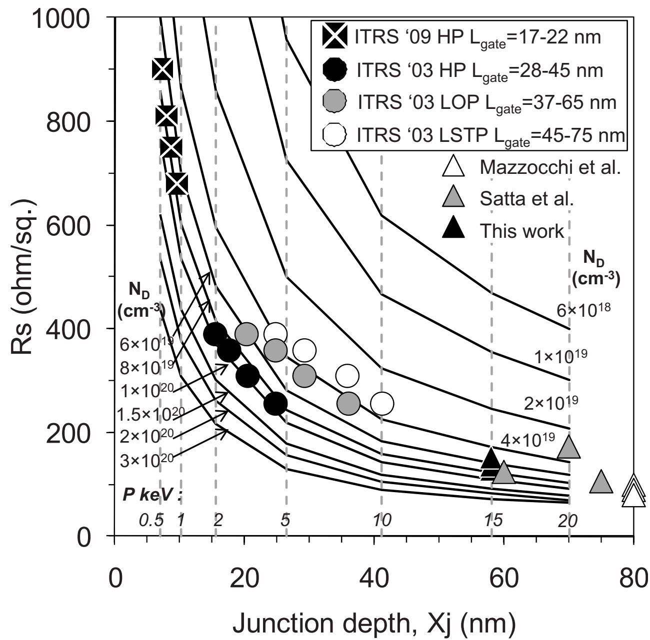

FIG. 3. R_s vs X_j for n-type germanium. Isolines are constructed with different maximum active concentrations for the P profiles shown in Fig. 2. The ITRS Roadmap specs are included from the 2009 and 2003 editions. Experimental data from this work, flash (Ref. 31), and laser (Ref. 26) anneal are shown, all for a 1×10^{15} cm^{-2} 15 keV P implant.

(LOP), and low-standby-power (LSTP) devices. Thus here R_s specs for LOP and LSTP are taken as those listed in the ITRS Roadmap for HP devices. X_j is a function of gate length (L_{gate}) which does change with device option. In Fig. 3 R_s versus X_j targets are separated for the 2003 ITRS HP, LOP, and LSTP devices. Clearly a higher active concentration is required for HP devices.

For the 2009 specs there was very little difference in targeted L_{gate} and X_j, thus for clarity only the most aggressive target is shown in Fig. 3. P implants followed by a diffusionless anneal, such as SPER, can meet the extended planar bulk ITRS specs for $L_{gate}=17-22$ nm with an active concentration of 8×10^{19} cm^{-3}. If a germanium-on-insulator or other thin-body germanium architecture is used for $L_{gate}=17-22$ nm, the resulting junction profiles can be assumed to be boxlike. The procedure of Fig. 3 was repeated for that case, and an active concentration of 6×10^{19} cm^{-3} was sufficient to hit the 2009 ITRS targets. Note, the plot is not shown here due to its similarity to Fig. 3.

In conclusion, the typical problems of n-type impurities in germanium such as diffusion, substrate loss, and outgassing can be overcome by using SPER for dopant activation. Recrystallization at 500 °C produced an active concentration of 7×10^{19} cm^{-3} which is in the order of that needed for sub-20 nm technologies.

This work has been funded by the Science Foundation Ireland under Research Grant No. 09/SIRG/I1623.

[1] *Germanium-Based Technologies*, edited by C. Claeys and E. Simoen (Elsevier, Amsterdam, 2007).
[2] H.-Y. Yu, S.-L. Cheng, P. B. Griffin, Y. Nishi, and K. C. Saraswat, IEEE Electron Device Lett. **30**, 1002 (2009).
[3] G. Hellings, J. Mitard, G. Eneman, B. De Jaeger, D. P. Brunco, D. Shamiryan, T. Vandeweyer, M. Meuris, M. M. Heyns, and K. De Meyer, IEEE Electron Device Lett. **30**, 88 (2009).
[4] L. Hutin, C. Le Royer, J.-F. Damlencourt, J.-M. Hartmann, H. Grampeix, V. Mazzocchi, C. Tabone, B. Previtali, A. Pouydebasque, M. Vinet, and O. Faynot, IEEE Electron Device Lett. **31**, 234 (2010).
[5] M. Caymax, G. Eneman, F. Bellenger, C. Merckling, A. Delabie, G. Wang, R. Loo, E. Simoen, J. Mitard, B. De Jaeger, G. Hellings, K. De Meyer, M. Meuris, and M. Heyns, Tech. Dig. - Int. Electron Devices Meet **2009**, 461.
[6] C. O. Chui, K. Gopalakrishnan, P. B. Griffin, J. D. Plummer, and K. C. Saraswat, Appl. Phys. Lett. **83**, 3275 (2003).
[7] C. O. Chui, L. Kulig, J. Moran, W. Tsai, and K. C. Saraswat, Appl. Phys. Lett. **87**, 091909 (2005).
[8] A. Satta, E. Simoen, R. Duffy, T. Janssens, T. Clarysse, A. Benedetti, M. Meuris, and W. Vandervorst, Appl. Phys. Lett. **88**, 162118 (2006).
[9] M. Koike, Y. Kamata, T. Ino, D. Hagishima, K. Tatsumura, M. Koyama, and A. Nishiyama, J. Appl. Phys. **104**, 023523 (2008).
[10] F. Priolo and E. Rimini, Mater. Sci. Rep. **5**, 319 (1990).
[11] R. Duffy, T. Dao, Y. Tamminga, K. van der Tak, F. Roozeboom, and E. Augendre, Appl. Phys. Lett. **89**, 071915 (2006).
[12] F. A. Trumbore, Bell Syst. Tech. J. **39**, 205 (1960).
[13] P. Pichler, *Intrinsic Point Defects, Impurities, and Their Diffusion in Silicon* (Springer, Berlin, 2004).
[14] N. Ioannou, D. Skarlatos, C. Tsamis, C. A. Krontiras, S. N. Georga, A. Christofi, and D. S. McPhail, Appl. Phys. Lett. **93**, 101910 (2008).
[15] A. Chroneos, D. Skarlatos, C. Tsamis, A. Christofi, D. S. McPhail, and R. Hung, Mater. Sci. Semicond. Process. **9**, 640 (2006).
[16] A. Satta, E. Simoen, T. Clarysse, T. Janssens, A. Benedetti, B. De Jaeger, M. Meuris, and W. Vandervorst, Appl. Phys. Lett. **87**, 172109 (2005).
[17] Y.-L. Chao, S. Prussin, J. C. S. Woo, and R. Scholz, Appl. Phys. Lett. **87**, 142102 (2005).
[18] G. Hellings, C. Wuendisch, G. Eneman, E. Simoen, T. Clarysse, M. Meuris, W. Vandervorst, M. Posselt, and K. De Meyer, Electrochem. Solid-State Lett. **12**, H417 (2009).
[19] E. Simoen, A. Brugère, A. Satta, A. Firrincieli, B. Van Daele, B. Brijs, O. Richard, J. Geypen, M. Meuris, and W. Vandervorst, J. Appl. Phys. **105**, 093538 (2009).
[20] Y.-L. Chao and J. C. S. Woo, IEEE Trans. Electron Devices **57**, 665 (2010).
[21] W. Lerch, S. Paul, J. Niess, F. Cristiano, Y. Lamrani, P. Calvo, N. Cherkashin, D. F. Downey, and E. A. Arevalo, J. Electrochem. Soc. **152**, G787 (2005).
[22] B. J. Pawlak, R. Surdeanu, B. Colombeau, A. J. Smith, N. E. B. Cowern, R. Lindsay, W. Vandervorst, B. Brijs, O. Richard, and F. Cristiano, Appl. Phys. Lett. **84**, 2055 (2004).
[23] N. E. B. Cowern, B. Colombeau, J. Benson, A. J. Smith, W. Lerch, S. Paul, T. Graf, F. Cristiano, X. Hebras, and D. Bolze, Appl. Phys. Lett. **86**, 101905 (2005).
[24] T. E. Haynes and O. W. Holland, Appl. Phys. Lett. **61**, 61 (1992).
[25] S. Koffel, P. Scheiblin, A. Claverie, and G. Benassayag, J. Appl. Phys. **105**, 013528 (2009).
[26] V. Mazzocchi, X. Pages, M. Py, J. P. Barnes, K. Vanormelingen, L. Hutin, R. Truche, P. Vermont, M. Vinet, C. Le Royer, and K. Yckache, *Proceedings of the 17th IEEE International Conference on Advanced Thermal Processing of Semiconductors—RTP 2009*, Albany (IEEE, New York, 2009), pp.1–5.
[27] A. Claverie, S. Koffel, N. Cherkashin, G. Benassayag, and P. Scheiblin, Thin Solid Films **518**, 2307 (2010).
[28] A. Chroneos, H. Bracht, R. W. Grimes, and B. P. Uberuaga, Mater. Sci. Eng., B **154–155**, 72 (2008).
[29] A. R. Peaker, V. P. Markevich, B. Hamilton, I. D. Hawkins, J. Slotte, K. Kuitunen, F. Tuomisto, A. Satta, E. Simoen, and N. V. Abrosimov, Thin Solid Films **517**, 152 (2008).
[30] G. M. Lopez, V. Fiorentini, G. Impellizzeri, S. Mirabella, and E. Napolitani, Phys. Rev. B **72**, 045219 (2005).
[31] A. Satta, A. D'Amore, E. Simoen, W. Anwand, W. Skorupa, T. Clarysse, B. van Daele, and T. Janssens, Nucl. Instrum. Methods Phys. Res. **257**, 157 (2007).
[32] The Stopping and Range of Ions in Matter, www.srim.org.
[33] V. I. Fistul, M. I. Iglitsyn, and E. M. Omel'yanovskii, Sov. Phys. Solid State **4**, 784 (1962).
[34] The International Technology Roadmap for Semiconductors, www.itrs.net.
[35] C. H. Poon, L. S. Tan, B. J. Cho, and A. Y. Du, J. Electrochem. Soc. **152**, G895 (2005).
[36] S. Heo, S. Baek, D. Lee, M. Hasan, H. Jung, J. Lee, and H. Hwang, Electrochem. Solid-State Lett. **9**, G136 (2006).